JACS
JOURNAL OF THE AMERICAN CHEMICAL SOCIETY
Article
pubs.acs.org/JACS

High-Temperature Ferroelectricity and Photoluminescence in a Hybrid Organic–Inorganic Compound: (3-Pyrrolinium)$MnCl_3$

Heng-Yun Ye,[†,‡] QiongHua Zhou,[⊥,‡] XiangHong Niu,[⊥] Wei-Qiang Liao,[†] Da-Wei Fu,[†] Yi Zhang,[†] Yu-Meng You,[*,†] Jinlan Wang,[*,⊥] Zhong-Ning Chen,[§] and Ren-Gen Xiong[*,†]

[†]Ordered Matter Science Research Center, Southeast University, Nanjing 211189, P. R. China
[⊥]Department of Physics, Southeast University, Nanjing 211189, P. R. China
[§]Fujian Institute of Research on the Structure of Matter, The Chinese Academy of Sciences, Fuzhou 350002, P. R. China

Supporting Information

ABSTRACT: Coupling of ferroelectricity and optical properties has become an interesting aspect of material research. The switchable spontaneous polarization in ferroelectrics provides an alternative way to manipulate the light–matter interaction. The recent observation of strong photoluminescence emission in ferroelectric hybrid organic–inorganic compounds, (pyrrolidinium)MnX_3 (X = Cl or Br), is an attractive approach to high efficiency luminescence with the advantages of ferroelectricity. However, (pyrrolidinium)MnX_3 only displays ferroelectricity near or below room temperature, which limits its future applications in optoelectronics and multifunctional devices. Here, we rationally designed and synthesized high-temperature luminescent ferroelectric materials. The new hybrid compound (3-pyrrolinium)$MnCl_3$ has a very high Curie temperature, T_c = 376 K, large spontaneous electronic polarization of 6.2 $\mu C/cm^2$, and high fatigue resistance, as well as high emission efficiency of 28%. This finding is a further step to the practical use of ferroelectric luminescence based on organic–inorganic compounds.

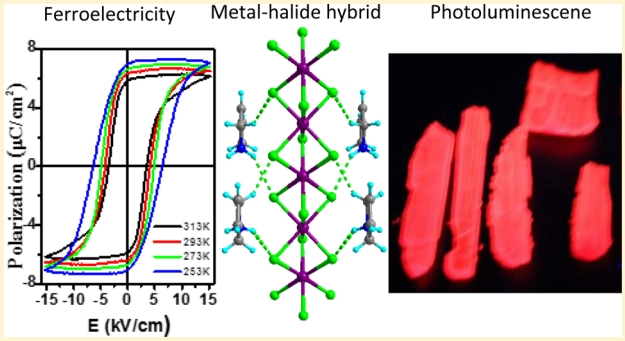

INTRODUCTION

Ferroelectricity has long been an attractive research area in the exploration of new materials. Analogous to ferromagnetism, the spontaneous electric polarization in ferroelectric materials can be reversed by an external electric field. Once combined with other material properties, such materials can be extremely useful in the application of photovoltaics, spintronics, optical–electrical–mechanical actuators, etc. On the other hand, research into ferroelectrics that also have the ability of light emitting is also a very interesting topic, because the introduction of spontaneous electric polarization can be a new way to manipulate the light–matter interactions. Such combination of luminescence and ferroelectricity leads to future multifunctional optoelectronic applications. Despite their significant potential, their practical application is still limited by the low light-emitting efficiency.[1] Conventional luminescent ferroelectrics are the rare-earth-doped perovskite-type materials. Due to the mechanism of such rare earth (RE) emissions, which rely on the effectiveness of energy transfer from the light-absorbing host to the RE activator, RE-doped luminescent ferroelectrics do not process very good emission efficiency.[1]

Previously, we reported an alternative approach to realize the coupling of ferroelectricity and luminescence with decent emission efficiency.[2] In the hybrid organic–inorganic ferroelectric compounds (pyrrolidinium)MnX_3 (X = Cl or Br), the photoluminescence (PL) quantum yield is as high as 28–56% under ultraviolet excitation with a lifetime of 157–515 μs. Such strong photoluminescence is attributed to a new energy-transfer-free mechanism. The activator is the octahedral Mn^{2+} ion, and the emission originates from the $(t_{2g})^3(e_g)^2-(t_{2g})^4(e_g)^1$ transition. The strategy in introducing the luminous activator is totally different from that in the RE-doped ferroelectrics. In conventional RE-doped ferroelectrics, the rare earth and the alkaline-earth ions jointly occupy the same lattice site with a specific ratio, and the concentration of the doped RE activator is limited to a narrow range, because higher or lower concentration will decrease the efficiency. For example, in Pr^{3+} doped $CaTiO_3$, the luminescence is systematically maximum for a Pr^{3+} with mole percentage of 0.2 and is quenched at 5 mol % after energy migration due to $Pr^{3+}-Pr^{3+}$ interaction.[1d,3] In the hybrid (pyrrolidinium)MnX_3, the activator Mn^{2+} ion occupies a lattice site completely, allowing enough luminous activators, and quenching can be avoided owing to the energy-transfer-free mechanism. Despite the high emission efficiency, there is still a roadblock toward practical luminescent ferroelectrics: Curie temperature (T_c). The T_c values of the previously reported compounds are below 300

Received: August 13, 2015
Published: September 18, 2015

DOI: 10.1021/jacs.5b08290
J. Am. Chem. Soc. 2015, 137, 13148–13154

K, which limits their application because one can only control the spontaneous polarization below room temperature.

In the course of exploring high-T_c ferroelectrics, we found that in the family of ABX_3 organo−metal halide ferroelectrics, a compound with 3-pyrrolinium has the highest T_c.[2,4] Inspired by this, in this work, we rationally synthesized (3-pyrrolinium)-$MnCl_3$ (**1**, Scheme 1), which is an isostructural compound of

Scheme 1. Structural Formula of Compound 1

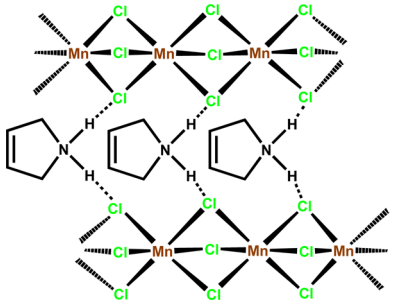

previously reported (pyrrolidinium)$MnCl_3$. Systematic characterization reveals that compound **1** has a significantly higher T_c and better ferroelectricity compared with its isostructural compound and, more importantly, a decent PL quantum yield.

MATERIALS AND METHODS

Synthesis. All reagents and solvents in the synthesis were purchased from Aladdin Chemistry Co., Ltd. (Shanghai, China). They were of reagent grade and used without further purification. Pink single crystals of compound **1** were grown by slow evaporation of a methanol solution (200 mL) containing equal molar amounts of 3-pyrrolinium chloride (100 mmol) and anhydrous manganese(II) chloride (100 mmol). The purity of the bulk phase was verified by the infrared spectrum (Supporting Information, Figure S1) and powder X-ray diffraction (Supporting Information, Figure S2).

Methods. Differential scanning calorimetry (DSC), second harmonic generation (SHG), dielectric, pyroelectric, polarization−electric field (P−E) hysteresis loops, and PL measurements were describe elsewhere.[5] For dielectric, ferroelectric, and pyroelectric measurements, the samples were made from single crystals cut into the form of thin plates perpendicular to the crystal *c*-axis with thickness of 0.5−1 mm and cross-sectional area of 5−10 mm^2.

RESULTS AND DISCUSSION

Ferroelectrics usually undergo temperature-triggered structural phase transitions from centrosymmetric high-temperature phases (HTPs) to noncentrosymmetric low-temperature phases (LTPs). To test whether there is such a structural phase transition in the crystalline material **1**, we performed DSC measurements. The DSC curve shows two reversible endothermic and exothermic peaks in heating and cooling runs (Figure 1), indicating a reversible phase transition at around T_c = 376 K. Ferroelectrics with such high T_c in recent emerging hybrid organic−inorganic ferroelectrics are rare.[6] The DSC peaks show broad precursory and tailing effects. This is because the transition is the order−disorder-type (see below) and was completed in a broad temperature range, as observed in the Cd analogue.[4b] The narrow thermal hysteresis and step-like peaks indicate the continuous character of a second-order transition.

For precise analysis of the main structural differences between the HTP and LTP and understanding the ferroelectric origin in compound **1**, we determined the crystal structures of the LTP and the HTP at 273 and 413 K, respectively, by X-ray

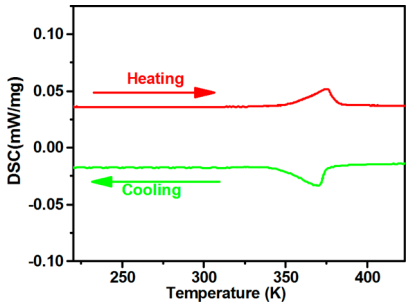

Figure 1. DSC curves for compound **1**, revealing a reversible phase transition.

diffraction.[7] The HTP is orthorhombic, space group *Cmcm*; the LTP assumed a polar space group $Cmc2_1$. They can be understood as the isostructures of our recently reported (pyrrolidinium)MnX_3 (X = Cl or Br) and (pyrrolidinium)-$CdCl_3$, respectively. It is known that a hybrid organic−inorganic perovskite ABX_3[8] may crystallize in a BX_6-corner-sharing cubic stacking structure, such as $CH_3NH_3PbX_3$, $CH_3NH_3SnX_3$, and $[(CH_3)_2NH_2][Cd(N_3)_3]$,[9] or in a BX_6-face-sharing hexagonal stacking structure, such as N-$(CH_3)_4CdBr_3$.[10] The crystal structure of compound **1** is of the BX_6-face-sharing hexagonal stacking case. It contains infinite columns of face-sharing $MnCl_6$ octahedra (Figure 2),

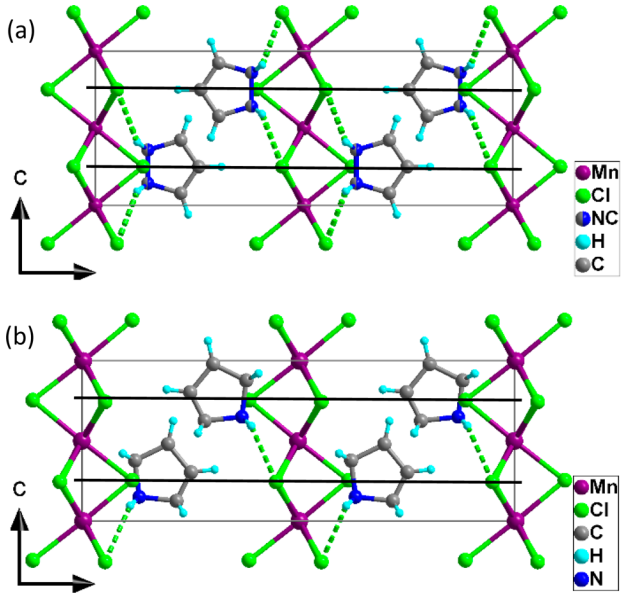

Figure 2. Projections of the crystal structures of compound **1** in the (a) HTP and (b) LTP down the common *a*-axis, showing the similarities of the lattices and differences of the orientational states of the cations. In panel a, the NC sites are occupied equally by the C and N atoms due to orientational disorder, and the presented model is the average of the two orientations. The dark lines indicate the crystallographic mirror planes in panel a and the pseudo-mirror planes in panel b.

arranged in the same manner as the NiO_6 units in the hexagonal 2-H $BaNiO_3$.[11] In both the HTP and the LTP, the coordination geometry of the central Mn atom is a quasi-regular octahedron; the configuration of the linear chains are comparable to those in other analogues, such as (pyrolidinium)$MnCl_3$,[2a] $(CH_3)_4NMnCl_3$,[12] and $(CH_3NH_3)MnCl_3$.[13] The cavities between the octahedral

DOI: 10.1021/jacs.5b08290
J. Am. Chem. Soc. 2015, 137, 13148−13154

columns are occupied by 3-pyrrolinium cations, analogous to the barium cations in $BaNiO_3$. In the HTP, the 3-pyrrolinium cation is located on the special position with 2*mm* symmetry. Although the 3-pyrrolinium cation possesses intermolecular 2*mm* symmetry with the N atom located on a 2-fold rotation axis, the intramolecular symmetry elements do not superimpose the crystallographic symmetry elements. The crystal symmetry requirement is satisfied by 2-fold orientational disorder with a C atom located on the crystallographic 2-fold axis, while the N atom distributes equally over the mirror plane in the [001] direction. The disorder leads to positive charges carried by the N atoms centered in the mirror planes. As shown in Figure S3 (Supporting Information), the elongated displacement ellipsoids of the C atoms indicate strong dynamics of the in-plane swing-like motion about the N atom fixed by N−H···Cl hydrogen-bonding interactions. Such molecular motion has been proven by solid state NMR experiments in the Cd analogure.[4b] In the LTP, the cationic ring plane remains located on the mirror plane in the [100] direction, while the mirror symmetry in the [001] direction is lost. It was refined as a single orientation. The molecular geometry (N1−C1 1.456(8), N1−C4 1.499(9), C1−C2 1.478(12), C2−C3 1.290(11), C3−C4 1.446(11) Å) points to a definitely ordered model. Thus, the transition is the order−disorder-type. As shown in Figure 2b, the ordered structure indicates that positive charges move down the *c*-axis. The average shift of the positive charges is about 0.8126 Å, which may induce polarization of 6.25 $\mu C/cm^2$, equal to the observed remnant polarization (6.2 $\mu C/cm^2$). This shows that the spontaneous polarization is contributed mainly by the ordering of the organic cations. With the similarities and differences of the HTP and LTP, one can understand the polarization reversal as realized mainly by the reorientation of the cations (Supporting Information, Figure S4).

To confirm the symmetry change in the transition, we measured the temperature dependent SHG response of compound **1**. For crystalline materials, the SHG signal can be observed only in noncentrosymmetric structures. A temperature-dependent SHG measurement on a polycrystalline sample is a simple but reliable method to confirm whether the sample undergoes a phase transition from a centrosymmetric phase to a noncentrosymmetric one. As shown in Figure 3, a strong signal was observable at room temperature. As temperature increases, the intensity decreases gradually and reaches zero at around T_c = 376 K. This indicates that the LTP is noncentrosymmetric, while the HTP is centrosymmetric,

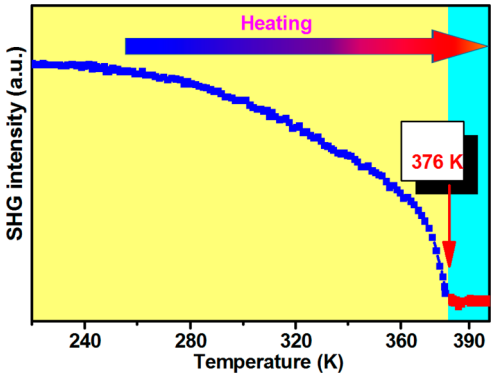

Figure 3. Temperature dependent SHG response of compound **1**, revealing a symmetry-breaking phase transition at around T_c = 376 K.

consistent with the crystal structure determination. The gradual decrease near T_c indicates that the transition is continuous.

The ferroelectric nature of the transition was proved by large dielectric anomalies. Structural phase transitions are usually accompanied by dielectric anomalies. Large dielectric anomalies are the characteristic of ferroelectric phase transitions.[14] As shown in Figure 4, the dielectric anomalies at frequency of 0.5

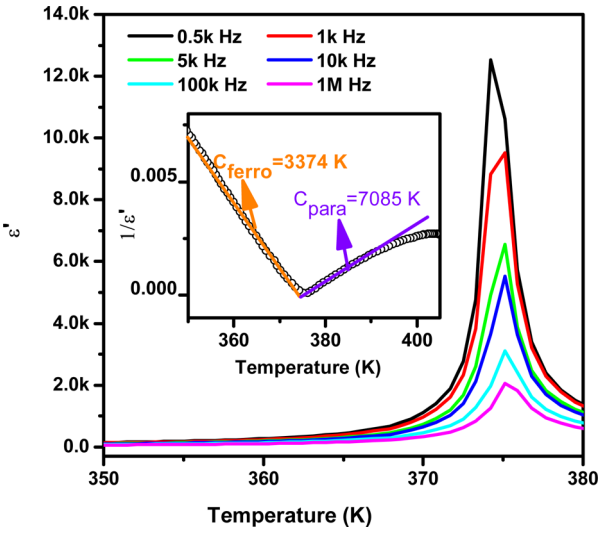

Figure 4. Real part of the complex dielectric constant of compound **1** as a function of temperature at several frequencies, measured along the polar *c*-axis of the LTP. Inset: Plot of $1/\varepsilon'$ vs temperature in the vicinity of T_c.

kHz to 1 MHz appear at around T_c. The peak values are a few thousand to ten thousand times larger than those at the stable state. As shown in the inset of Figure 4, the dielectric response shows Curie−Weiss behavior in the vicinity of T_c, $\varepsilon' = C_{para}/(T - T_0)$ $(T > T_c)$ or $C_{ferro}/(T_{0'} - T)$ $(T < T_c)$, where C_{para} and C_{ferro} are the Curie constants and T_0 and $T_{0'}$ are the Curie−Weiss temperatures for the paraelectric and ferroelectric phases, respectively, which is further evidence for a proper ferroelectric phase transition. The fitted Curie constants at 500 Hz are C_{para} = 7085 K and C_{ferro} = 3374 K, and the Curie−Weiss temperatures are $T_0 \approx T_{0'}$ = 376.3 K. The C_{para}/C_{ferro} ratio of 2.0 agrees well with the theoretical value $(C_{para}/C_{ferro} = 2)$ expected for a second-order ferroelectric phase transition.[15] Curie constants fitted at other frequencies are given in the Supporting Information, Table S1.

Besides large dielectric anomalies, ferroelectrics, as a special class of dielectrics, show strong nonlinear dielectric response due to switchable spontaneous polarization. We investigated such a property by measuring the bias field dependent dielectric constant. As shown in Figure 5, in the HTP at 383 K, the dielectric response remains constant when the applied external field is switched, while in the LTP, it shows butterfly like peaks at various temperatures, as observed for other well studied ferroelectrics.[16] These behaviors correspond to those for ordinary dielectrics and ferroelectrics, respectively, suggesting that the HTP at 383 K is a paraelectric phase and the LTP below 373 K is a ferroelectric phase.

The properties of ferroelectric switchable polarization are investigated by measuring polarization hysteresis loops. The results are illustrated in Figure 6. Figure 6a presents the hysteresis loops at various temperatures at 50 Hz. The well-

DOI: 10.1021/jacs.5b08290
J. Am. Chem. Soc. 2015, 137, 13148−13154

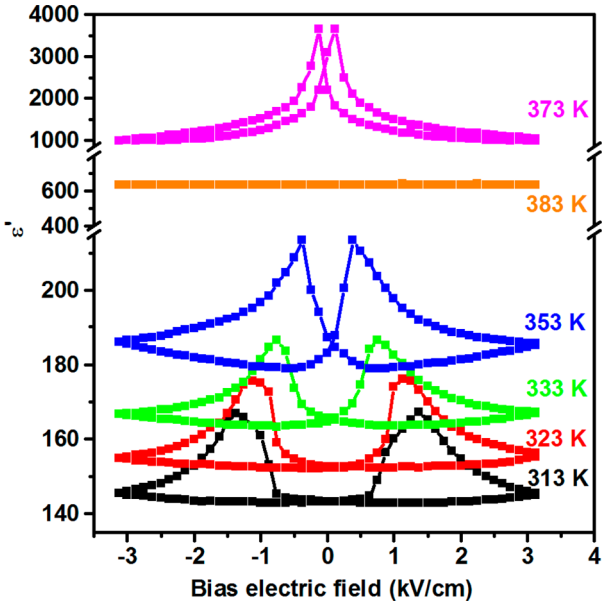

Figure 5. Bias-field-dependent ε' of compound **1**, measured along the *c*-axis at various temperatures.

opened loops can be considered as direct evidence for ferroelectricity. At room temperature, 293 K, the observed saturated polarization (P_s) and remnant polarization (P_r) are almost equal, 6.2 μC/cm^2, a little greater than those for the isostructural (pyrrolidinium)MnX_3 (X = Cl or Br) and (3-pyrrolinium)$CdCl_3$ (4.5−6.0 μC/cm^2). P_s is among the highest values observed for molecular ferroelectrics.[5a,6,17] The coercive field (E_c) is 2.5 kV/cm, comparable to those for the isostructural compounds. These similarities corroborate the assignment of a similar ferroelectric mechanism for them. Figure 6b presents the hysteresis loops at various applied fields at room temperature. As frequency increases, P_r decreases and E_c increases gradually. The hysteresis loop retains high rectangularity at frequency as high as 20 kHz, showing excellent polarization switching performance. Molecular ferroelectrics with such a high working frequency are rare. Good rectangularity at high frequency is desirable for applications such as memory, which need high speed reversal operation. The excellent polarization switching performance was also tested in the fatigue measurement. It is interesting to find that P_r and P_s reduced no more than 50% after switching operation 1×10^8 times, showing good fatigue resistance (Figure 6c). These excellent ferroelectric properties may find application in device applications, such as memory.

The spontaneous polarization was further evaluated by the Berry phase method developed by Kingsmith and Vanderbilt.[18] The first-principles calculations were performed within the framework of density functional theory (DFT) implemented in

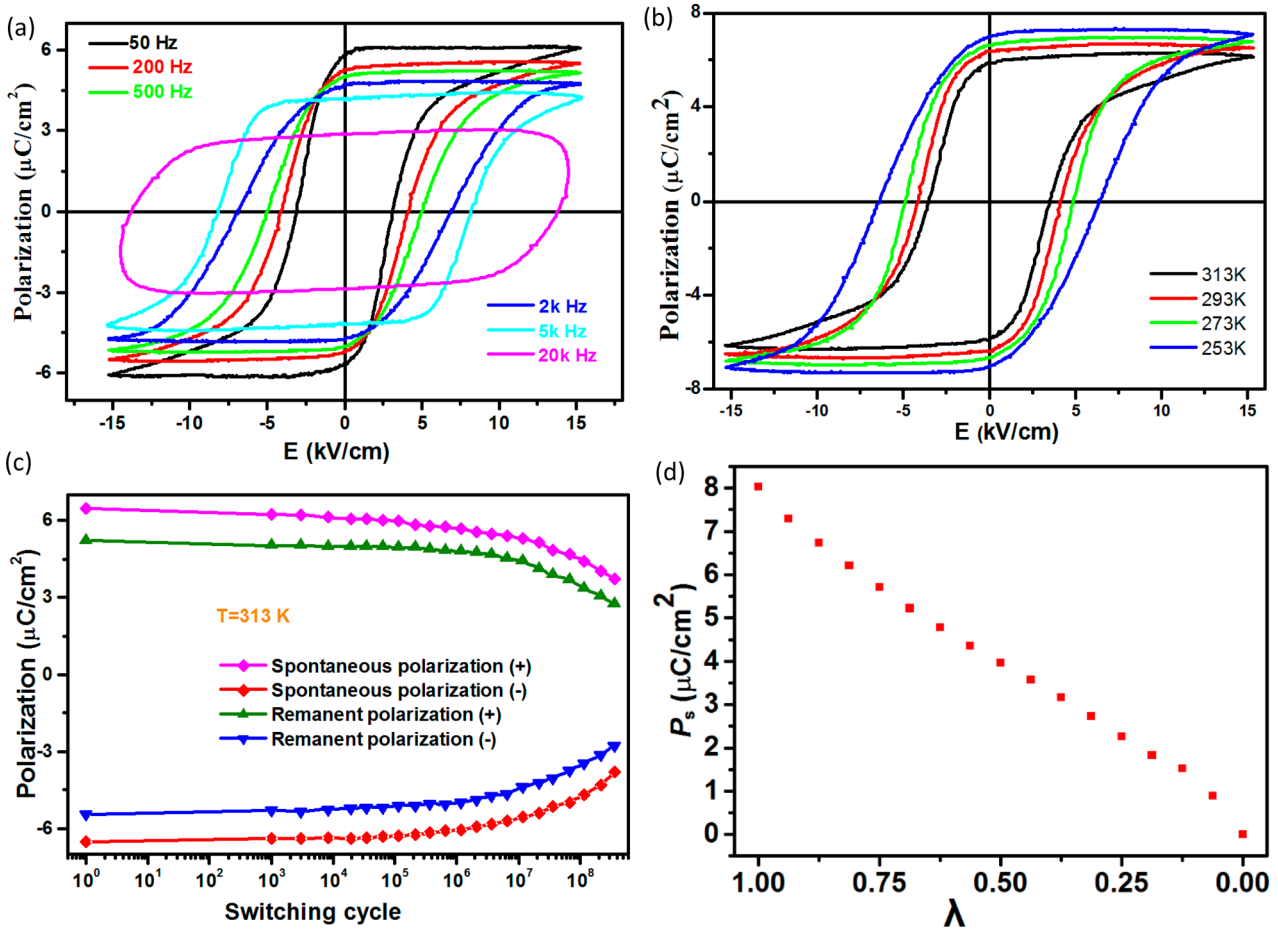

Figure 6. Ferroelectric properties of compound **1**. (a, b) Ferroelectric hysteresis loops measured along the polar *c*-axis of the LTP at different temperatures and frequencies, showing excellent reversibility. (c) Polarization change as the measured cycle, showing high fatigue resistance. (d) PBE ferroelectric polarization along the path connecting the centrosymmetric structure (λ = 0) to the optimized polar structure (λ = 1).

DOI: 10.1021/jacs.5b08290
J. Am. Chem. Soc. 2015, 137, 13148−13154

the Vienna *ab initio* Simulation Package (VASP).[19] The exchange−correlation interactions were treated within the generalized gradient approximation of the Perdew−Burke−Ernzerhof type.[20] The ground state of the experimental room temperature ferroelectric structure is found to be antiferromagnetic along the $MnCl_3$ chain with a magnetic moment of 4.4 μ_B for each Mn atom, which is 0.16 eV per unit cell lower than the ferromagnetic state. The calculated polarization along the *c*-axis is about 6.87 $\mu C/cm^2$, which reproduces the experimental value of 6.20 $\mu C/cm^2$. Then we allowed the atoms to relax until atomic forces on each atom are smaller than 0.01 eV/Å. The polarization of this optimized structure is about 8.04 $\mu C/cm^2$, and a larger polarization below the room temperature can be expected. The continuous evolution of spontaneous polarization from the centrosymmetric structure ($\lambda = 0$) to the optimized polar structure ($\lambda = 1$) is plotted as a function of dimensionless parameter λ in Figure 6d. Both the displacement and the rotation of 3-pyrrolinium cations are implied in λ.

As expected, compound **1** emits PL in the solid state. Under ultraviolet excitation, it emits bright orange-red light, as observed in (pyrrolidinium)$MnCl_3$[2a] and $(CH_3)_4NMnCl_3$.[12,21] The absorption and emission spectra are illustrated in Figure 7. Eight absorption peaks at around 537, 444, 425, 375, 358, 326, 265, and 244 nm are distinguished. The six labeled absorptions in the range of 300−600 nm are comparable to those of (pyrrolidinium)$MnCl_3$ and $(CH_3)_4NMnCl_3$.[21a] Since all three compounds have similar crystal structures (Figure S5, Supporting Information), the similar absorptions should correspond to the same electronic transitions. As revealed for $(CH_3)_4NMnCl_3$, these absorptions can be ascribed to electronic transitions between the ground and the excited states of the Mn^{2+} ion in an octahedral crystal field.[21a] The absorption peak at 537 nm nearest to the emission peak corresponds to a transition from the ground state of the d-electron configuration $(t_{2g})^3(e_g)^2$ to the upper state of the configuration $(t_{2g})^4(e_g)^1$.[21] The other two peaks at 265 and 244 nm thus originate from the transitions within the 3-pyrrolinium cation, including the $\pi-\pi^*$ and $\sigma-\pi^*$. The emission peak is centered at around 635 nm. The large energy separation between the emission maximum, 635 nm, and the nearest absorption maximum, 537 nm, is probably due to the forbidden transition from the ground sextet to the first excited level.[21a] For compound **1** and (pyrrolidinium)$MnCl_3$, similar crystal structures and the same mechanism of PL suggest a similar emission efficiency in PL. However, the quantum yield (28.22%) (Supporting Information, Figure S6) and lifetime (333.6 μs) (Supporting Information, Figure S7) of compound **1** at room temperature are significantly lower and shorter than those for (pyrrolidinium)$MnCl_3$, respectively.

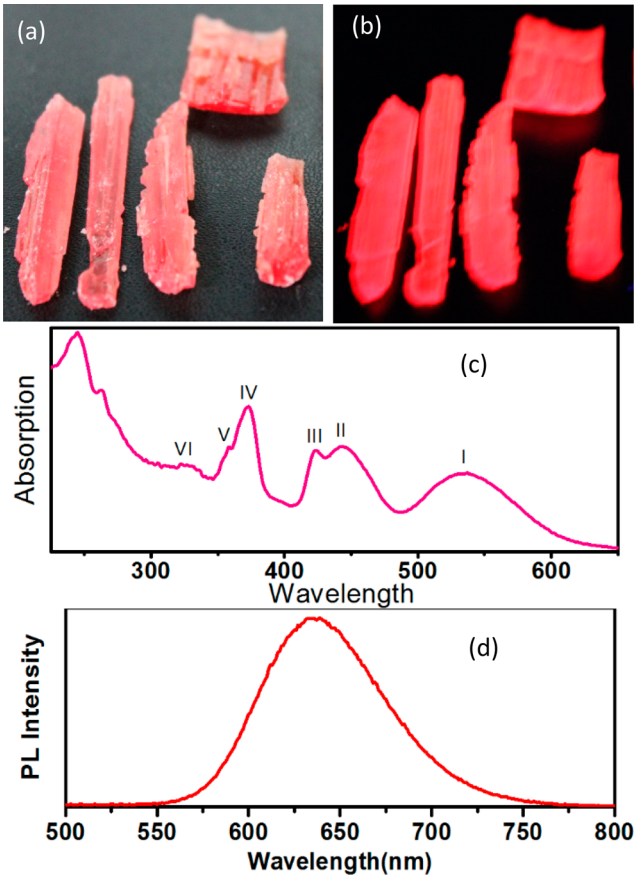

Figure 7. (a) Pink crystals of compound **1** under ambient light. (b) Orange-red PL of compound **1** under UV light. (c, d) Absorption and emission spectra of compound **1** at room temperature.

To reveal the higher quantum yield of 56% for (pyrrolidinium)$MnCl_3$[2a] compared with that of 28.2% for compound **1**, we performed first principle calculations for both crystals. The crystal structures of these two compounds are very similar, and the only difference between them is that there is a double bond in the 3-pyrrolinium cation, while the pyrrolidinium cation is fully saturated. The structures determined experimentally only show a negligible difference in cell constants due to the nonequivalent steric hindrance of carbon−hydrogen bonds. The ground state of (pyrrolidinium)-$MnCl_3$, which is antiferromagnetic with a magnetic moment of 4.4 μ_B for each Mn atom and has a spontaneous polarization of 8.04 $\mu C/cm^2$, shows no difference with that of (3-pyrrolinium)-$MnCl_3$ (Table S2). The band structures of both crystals [together with their corresponding densities of states (DOSs)] and the highest occupied band and lowest unoccupied band are presented in Figure S8 (Supporting Information). One can see that for both structures, bands near the Fermi level (E_F) are mainly dominated by Mn. Its strongly localized feature suggests that the luminescence of both structures is mainly produced by the octahedrally coordinated Mn ion. The DOS of the 3-pyrrolinium cation appears 4 eV above E_F and 1.5 eV below E_F originating from the double bond, but it should have no influence on the red phosphorescence at 635 nm, because it is too deep. Since the $MnCl_3$ is responsible for the luminescence, different cations only influence it in an indirect way. We calculate the charge transferred from the molecular cation to the $MnCl_3$ anion by Bader charge analysis.[22] It turns out that there was no significant difference between (pyrrolidinium)-$MnCl_3$ and (3-pyrrolinium)$MnCl_3$, even when van der Waals interactions were considered. Because quantum yield is also affected by many extrinsic properties such as defects, impurities, morphology, surface absorbance, and grain boundaries, we believe the crystal quality plays a very important role here. In this circumstance, crystals of (pyrrolidinium)$MnCl_3$ should have a better quality than that of compound **1**, possibly due to the differences in chemical composition.

Furthermore, ferroelectric PL has been observed to be sensitive to electric polarization because of polarization-induced lattice field changes or local environmental perturbations. It is expected that the PL in compound **1** can be affected to some

DOI: 10.1021/jacs.5b08290
J. Am. Chem. Soc. 2015, 137, 13148−13154

extent by varying the electric polarization. However, a preliminary study by using an external field of 5 kV/cm on the sample shows that the external field affects the phosphorescence of compound **1** negligibly (results not shown).

CONCLUSION

In summary, combination of high-T_c ferroelectricity and high quantum-yield PL was realized in hybrid (3-pyrrolinium)-$MnCl_3$. This opens an alternative avenue to prepare new luminescent ferroelectrics, which are different from the luminous activator-doped host materials. The characteristic of the structural tunability of hybrid materials also provides great flexibility in their ferroelectric luminescent properties. Higher quantum yield is expected by growing high-quality crystals. Because of the excellent above-room-temperature ferroelectricity and efficient PL, (3-pyrrolinium)$MnCl_3$ would be an attractive candidate for use of hybrid organic−inorganic compounds as multifunctional ferroelectric devices.

ASSOCIATED CONTENT

Supporting Information

The Supporting Information is available free of charge on the ACS Publications website at DOI: 10.1021/jacs.5b08290.

Low-temperature structure of (3-pyrrolinium)$MnCl_3$ (CIF)

High-temperature structure of (3-pyrrolinium)-$MnCl_3$(CIF)

IR spectrum, powder X-ray diffraction, and ellipsoid representations of symmetric units at high and low temperature of (3-pyrrolinium)$MnCl_3$, schematic drawing of polarization reversal in (3-pyrrolinium)$MnCl_3$, comparison of crystal structures of (tetramethylammonium)$MnCl_3$, (pyrrolidinium)$MnCl_3$, and (3-pyrrolinium)$MnCl_3$, measurement of quantum yield and lifetime of (3-pyrrolinium)$MnCl_3$, band structure and density of states of (pyrrolidinium)$MnCl_3$ and (3-pyrrolinium)$MnCl_3$, fitted Curie constants at different frequencies, and comparison between ground states of (pyrrolidinium)$MnCl_3$ and (3-pyrrolinium)-$MnCl_3$ (PDF)

AUTHOR INFORMATION

Corresponding Authors

*xiongrg@seu.edu.cn

*jlwang@seu.edu.cn

*youyumeng@seu.edu.cn

Author Contributions

‡H.-Y.Y. and Q.Z. contributed equally to this work.

Notes

The authors declare no competing financial interest.

ACKNOWLEDGMENTS

This work was supported by 973 project (Grant 2014CB932103) and the National Natural Science Foundation of China (Grants 21290172, 91422301, and 21427801).

REFERENCES

(1) (a) Okamoto, S.; Kobayashi, H.; Yamamoto, H. *J. Appl. Phys.* **1999**, *86*, 5594. (b) Diallo, P. T.; Boutinaud, P.; Mahiou, R.; Cousseins, J. C. *Phys. Stat. Sol. (a)* **1997**, *160*, 255. (c) Pizani, P. S.; Leite, E. R.; Pontes, F. M.; Paris, E. C.; Rangel, J. H.; Lee, E. J. H.; Longo, E.; Delega, P.; Varela, J. A. *Appl. Phys. Lett.* **2000**, *77*, 824. (d) Yamamoto, H.; Okamoto, S.; Kobayashi, H. *J. Lumin.* **2002**, *100*, 325.

(2) (a) Zhang, Y.; Liao, W. Q.; Fu, D. W.; Ye, H. Y.; Chen, Z. N.; Xiong, R. G. *J. Am. Chem. Soc.* **2015**, *137*, 4928. (b) Zhang, Y.; Liao, W. Q.; Fu, D. W.; Ye, H. Y.; Liu, C. M.; Chen, Z. N.; Xiong, R. G. *Adv. Mater.* **2015**, *27*, 3942.

(3) Diallo, P. T.; Jeanlouis, K.; Boutinaud, P.; Mahiou, R.; Cousseins, J. C. *J. Alloys Compd.* **2001**, *323-324*, 218.

(4) (a) Zhang, Y.; Ye, H.-Y.; Zhang, W.; Xiong, R.-G. *Inorg. Chem. Front.* **2014**, *1*, 118. (b) Ye, H.-Y.; Zhang, Y.; Fu, D.-W.; Xiong, R.-G. *Angew. Chem., Int. Ed.* **2014**, *53*, 11242.

(5) (a) Ye, H. Y.; Li, S. H.; Zhang, Y.; Zhou, L.; Deng, F.; Xiong, R. G. *J. Am. Chem. Soc.* **2014**, *136*, 10033. (b) Zhang, Y.; Liu, Y. M.; Ye, H. Y.; Fu, D. W.; Gao, W. X.; Ma, H.; Liu, Z. G.; Liu, Y. Y.; Zhang, W.; Li, J. Y.; Yuan, G. L.; Xiong, R. G. *Angew. Chem., Int. Ed.* **2014**, *53*, 5064.

(6) Zhang, W.; Xiong, R. G. *Chem. Rev.* **2012**, *112*, 1163.

(7) Crystal data for **1** at 413 K: $C_4H_8Cl_3MnN$, M_r = 231.40, orthorhombic, *Cmcm*, a = 7.470(15) Å, b = 17.64(4) Å, c = 6.515(12) Å, V = 859(3) Å^3, Z = 4, D_c = 1.790 g cm^{-3}, $R_1(I > 2\sigma(I))$ = 0.0301, wR_2(all data) = 0.0828, μ = 2.387 mm^{-1}, S = 1.110. At 273 K: orthorhombic, *Cmc*21, a = 7.361(5) Å b = 17.490(11) Å c = 6.466(4) Å, V = 832.4(9) Å^3, Z = 4, D_c = 1.846 g cm^{-3}, $R_1(I > 2\sigma(I))$ = 0.0204, wR_2(all data) = 0.0521, μ = 2.463 mm^{-1}, S = 1.070.

(8) (a) Katz, L.; Ward, R. *Inorg. Chem.* **1964**, *3*, 205. (b) Darriet, J.; Subramanian, M. A. *J. Mater. Chem.* **1995**, *5*, 543.

(9) (a) Onodayamamuro, N.; Matsuo, T.; Suga, H. *J. Chem. Thermodyn.* **1991**, *23*, 987. (b) Takahashi, Y.; Obara, R.; Lin, Z. Z.; Takahashi, Y.; Naito, T.; Inabe, T.; Ishibashi, S.; Terakura, K. *Dalton Trans.* **2011**, *40*, 5563. (c) Yamada, K.; Kuranaga, Y.; Ueda, K.; Goto, S.; Okuda, T.; Furukawa, Y. *Bull. Chem. Soc. Jpn.* **1998**, *71*, 127. (d) Du, Z. Y.; Xu, T. T.; Huang, B.; Su, Y. J.; Xue, W.; He, C. T.; Zhang, W. X.; Chen, X. M. *Angew. Chem., Int. Ed.* **2015**, *54*, 914. (e) Du, Z. Y.; Zhao, Y. P.; Zhang, W. X.; Zhou, H. L.; He, C. T.; Xue, W.; Wang, B. Y.; Chen, X. M. *Chem. Commun.* **2014**, *50*, 1989.

(10) Gesi, K. *J. Phys. Soc. Jpn.* **1990**, *59*, 432.

(11) Lander, J. J. *Acta Crystallogr.* **1951**, *4*, 148.

(12) Morosin, B.; Graeber, E. J. *Acta Crystallogr.* **1967**, *23*, 766.

(13) Bachmann, W.; Oswald, H. R.; Gunter, J. R. *J. Appl. Crystallogr.* **1976**, *9*, 243.

(14) Lines, M. E.; Glass, A. M. *Principles and Applications of Ferroelectrics and Related Materials*; Clarendon Press: Oxford, 1977.

(15) Rabe, K. M., Ahn, C. H., Triscone, J.-M., Eds. *Physics of Ferroelectrics—A Modern Perspective*; Springer: Berlin, 2007.

(16) Chen, W.; Yao, X.; Wei, X. Y. *Solid State Commun.* **2007**, *141*, 84.

(17) (a) Fu, D. W.; Cai, H. L.; Liu, Y. M.; Ye, Q.; Zhang, W.; Zhang, Y.; Chen, X. Y.; Giovannetti, G.; Capone, M.; Li, J. Y.; Xiong, R. G. *Science* **2013**, *339*, 425. (b) Fu, D. W.; Zhang, W.; Cai, H. L.; Ge, J. Z.; Zhang, Y.; Xiong, R. G. *Adv. Mater.* **2011**, *23*, 5658. (c) Fu, D. W.; Zhang, W.; Cai, H. L.; Zhang, Y.; Ge, J. Z.; Xiong, R. G.; Huang, S. D. *J. Am. Chem. Soc.* **2011**, *133*, 12780. (d) Fu, D. W.; Cai, H. L.; Li, S. H.; Ye, Q.; Zhou, L.; Zhang, W.; Zhang, Y.; Deng, F.; Xiong, R. G. *Phys. Rev. Lett.* **2013**, *110*, 257601. (e) Zhang, Y.; Zhang, W.; Li, S. H.; Ye, Q.; Cai, H. L.; Deng, F.; Xiong, R. G.; Huang, S. P. D. *J. Am. Chem. Soc.* **2012**, *134*, 11044. (f) Horiuchi, S.; Kagawa, F.; Hatahara, K.; Kobayashi, K.; Kumai, R.; Murakami, Y.; Tokura, Y. *Nat. Commun.* **2012**, *3*, 1308. (g) Sun, Z. H.; Chen, T. L.; Luo, J. H.; Hong, M. C. *Angew. Chem., Int. Ed.* **2012**, *51*, 3871. (h) Di Sante, D.; Stroppa, A.; Jain, P.; Picozzi, S. *J. Am. Chem. Soc.* **2013**, *135*, 18126. (i) Xu, G. C.; Zhang, W.; Ma, X. M.; Chen, Y. H.; Zhang, L.; Cai, H. L.; Wang, Z. M.; Xiong, R. G.; Gao, S. *J. Am. Chem. Soc.* **2011**, *133*, 14948. (j) Akutagawa, T.; Koshinaka, H.; Sato, D.; Takeda, S.; Noro, S.; Takahashi, H.; Kumai, R.; Tokura, Y.; Nakamura, T. *Nat. Mater.* **2009**, *8*, 342.

(18) (a) Kingsmith, R. D.; Vanderbilt, D. *Phys. Rev. B: Condens. Matter Mater. Phys.* **1993**, *47*, 1651. (b) Vanderbilt, D.; Kingsmith, R. D. *Phys. Rev. B: Condens. Matter Mater. Phys.* **1993**, *48*, 4442.

DOI: 10.1021/jacs.5b08290
J. Am. Chem. Soc. 2015, 137, 13148−13154

(19) (a) Kresse, G.; Furthmuller, J. *Phys. Rev. B: Condens. Matter Mater. Phys.* **1996**, *54*, 11169. (b) Kresse, G.; Furthmuller, J. *Comput. Mater. Sci.* **1996**, *6*, 15.
(20) Perdew, J. P.; Burke, K.; Ernzerhof, M. *Phys. Rev. Lett.* **1996**, *77*, 3865.
(21) (a) Lawson, K. E. *J. Chem. Phys.* **1967**, *47*, 3627. (b) Orgel, L. E. *J. Chem. Phys.* **1955**, *23*, 1958. (c) Orgel, L. E. *J. Chem. Phys.* **1955**, *23*, 1824.
(22) Bader, R. *Atoms in Molecules: A Quantum Theory*; Oxford University Press: New York, 1990.

DOI: 10.1021/jacs.5b08290
J. Am. Chem. Soc. 2015, 137, 13148−13154